

Electroperturbation of the human skin barrier in vitro (I): the influence of current density on the thermal behaviour of skin impedance¹

W.H.M. Craane-van Hinsberg, J.C. Verhoef, H.E. Junginger*, H.E. Boddé

*Leiden/Amsterdam Center for Drug Research, Division of Pharmaceutical Technology, Leiden University, P.O. Box 9502,
2300 RA Leiden, The Netherlands*

Received 12 February 1995; accepted 19 June 1996

Abstract

The effects of current density on the temperature dependence of the electrical properties of human stratum corneum were investigated in vitro at two different current densities: 13 and 130 $\mu\text{A cm}^{-2}$. To obtain information on the structural basis of the current-induced effects on the electrical resistances and capacitances, stratum corneum samples were subjected to three heating-and-cooling cycles (20–45–20°C; 20–75–20°C and 20–95–20°C) which included four lipid phase transitions. At both current densities three characteristic temperature intervals could be distinguished: (1) A lower interval, from 20 to about 60°C at the lower current density and from 20 to about 50°C at the higher current density. In this interval a constant activation energy for ion transport and a gradual decrease of the resistances were found, whereas the capacitances were almost constant; all changes within this interval were thermo-reversible; (2) A middle interval, from 60 to about 75°C at the lower and from 50 to about 75°C at the higher current density. Within these temperature ranges, a rapid and thermo-irreversible decrease of the resistances was observed, accompanied by an increase of the capacitances; and (3) A higher interval, from 75 to 95°C, within which the resistance did not decrease any further, although the capacitance increase continued. At a current density of 13 $\mu\text{A cm}^{-2}$, the activation energy of ion transport across human stratum corneum was $5.4 \pm 0.7 \text{ kcal mol}^{-1}$, which suggested the presence of highly conductive pathways. The middle temperature interval at 13 $\mu\text{A cm}^{-2}$, 60–75°C, in which irreversible changes occurred, corresponded with the temperature interval of the gel-liquid phase transition of stratum corneum lipids. The irreversible increase of the capacitances further continued from 75 to 95°C. Hence, the capacitances are determined by free lipids as well as protein-bound lipids. At 130 $\mu\text{A cm}^{-2}$ the temperature dependence of the electrical properties had the same features as observed at 13 $\mu\text{A cm}^{-2}$, but with two important differences: (1) A 15-fold decrease of the activation energy to $0.37 \pm 0.03 \text{ kcal mol}^{-1}$; and (2) A downward shift by almost 10°C of the temperature, at which the thermal transition of the electrical properties starts. In conclusion, the thermal analysis of electrical properties has shown that the resistances of human stratum corneum are closely associated with the intercellular lipid lamellae, whereas the capacitances are determined by both the intercellular lipid lamellae and protein-bound lipids. Furthermore, under influence of an electrical field the lipid phase transition temperature is shifted downward, indicating that the electrical field is capable of modifying the arrangements of stratum corneum lipids. © 1997 Elsevier Science B.V. All rights reserved

Keywords: Iontophoresis; Human stratum corneum; Skin capacitance; Skin impedance; Skin thermal analysis

1. Introduction

In recent years the transdermal route of administration has been investigated as an alternative for the delivery of peptide drugs, which compounds cannot be

* Corresponding author.

¹ Dedicated to Dr P. Reisen, former president of APV.

delivered effectively by the conventional peroral route and have to be administered by parenteral injections [1]. However, the permeability of the skin to hydrophilic and macromolecular peptide drugs is extremely low, and to achieve therapeutic drug levels, the use of iontophoresis is a very promising approach [2–4]. An important aspect of transdermal iontophoresis is that the rate of delivery of drugs can be controlled within narrow limits, if desired adjusted periodically, or even preprogrammed [5].

It has been found that, among other models with R||C-circuits [6], the electrical properties of the stratum corneum of the skin can be satisfactorily modelled by a series connection of two R||C-circuits [7,8]. It should be stated, however, that both the models described in the literature and our model consisting two R||C-circuits in series as adapted from Lykken [7] are only approximations to describe the electrical properties of the skin [9]. The two resistances determine the magnitude of the electrical barrier, while the capacitances are a measure of the charge storage capacity of stratum corneum. Previous studies have revealed that the structural basis for both the resistance and the capacitance properties of the human skin can largely be found in the intercellular lipids of stratum corneum [10,11]. In these studies thermal analysis of the electrical resistances and capacitances was performed at a current density low enough to cause no changes of the electrical resistance or capacitance [11]. The observation was made that the resistances as well as the capacitances abruptly change at the gel-liquid phase transition temperature between 65 and 75°C. On that account, the resistances and capacitances were attributed to the unbound skin lipids, organised in a lamellar phase. Unlike the resistances, the capacitances were found to be determined by protein-bound lipids as well, which undergo a phase transition at 85°C.

The structural changes which are responsible for observed increase in electrical skin conductance and permeability during iontophoresis are still under debate. The fact that the electrical resistances and capacitances of human stratum corneum are largely determined by the intercellular lipid lamellae led us to hypothesise that the electrical perturbation of the electrical properties of stratum corneum would involve, like the thermal perturbation, changes in the ordering of the intercellular lipids. To find out whether indeed current-induced changes of the resistances or capacitances are related to changes in lipid structures of stratum corneum, temperature was used as an auxiliary parameter, determining the nature and degree of lipid ordering in stratum corneum. For this purpose thermal analysis of the human stratum corneum resistances and capacitances was performed at two different current densities: a low non-perturbing current density and a high one, which is capable of perturbing the electrical properties

[12]. The findings of the present study concentrate on excised human stratum corneum and do not take into account possible influences of skin appendages.

2. Materials and methods

2.1. Isolation of stratum corneum

Stratum corneum was isolated from human abdomen skin within 24 h after the surgical correction. The following experiments were performed with skin samples obtained from a single 40 year old female donor. The subcutaneous fat was removed and the skin was dermatomed to a thickness of 300 μm . Then the dermatomed skin was spread with its dermal side on a piece of Whatman paper, which was wetted with 0.15 M phosphate buffered saline (PBS) of pH 7.4 containing 0.2% trypsin (type III; bovine; Sigma). Bidistilled water was used for the preparation of PBS. The buffer was composed of 0.149 M NaCl, 2 mM KH_2PO_4 and 2 mM NaHPO_4 , and adjusted to a pH value of 7.4 with phosphoric acid. The skin was incubated overnight on the enzyme solution at 4°C and subsequently incubated at 37°C for 1 h. The stratum corneum was carefully peeled off from the underlying cells using tweezers. To prevent further enzymatical degradation, the stratum corneum was bathed for several min in a 0.2% solution of trypsin-inhibitor (type II-S from soybean; Sigma) in PBS pH 7.4, then washed three times in bidistilled water and subsequently dried in a desiccator over silica gel and under nitrogen gas to prevent oxidation of lipids.

2.2. Stratum corneum hydration

Stratum corneum was punched into disks of 16 mm diameter, which were placed on a plastic grid above 0.15 M PBS for 48 h at 4°C. Then the samples were mounted in the transport cells described below, which were filled with 0.15 M PBS (pH 7.4). The stratum corneum samples were allowed to equilibrate in the buffer for 2 h at 20°C before experiments were started.

2.3. Transport cells

Transport cells were developed in the Mechanical Department of the Gorlaeus Laboratories (Leiden University, Netherlands). They were constructed from perspex and consisted of two compartments, between which a piece of stratum corneum was mounted, leaving an area of 0.79 cm^2 for transport [12]. Both compartments were filled with 0.15 M PBS pH 7.4 and connected to a circulating system. Buffer was transported from a glass reservoir to the transport cells by a peristaltic pump (Ismatec IPS-8, Zürich, Switzerland)

equipped with Tygon tubes (Ismatec, type ENE20, 0.073 inch inner diameter). The transport cells and glass reservoir were placed in a programmable waterbath (type SW1, Julabo Labortechnik, Seelbach, Germany). The temperature of the skin was monitored by two NiCr-Ni thermo-sensors (Shimaden Sr35-3111, Japan), placed 0.5 mm from each skin surface. The temperature of the waterbath was kept constant within 0.1 K from the desired temperature for isothermic experiments; for heating-cooling cycles the temperature of the waterbath was changed at a rate of 2.5 K min⁻¹.

2.4. Experimental protocol

For each of the two current densities used (13 and 130 $\mu\text{A cm}^{-2}$, respectively), the following protocols were used:

2.4.1. Measurements at 20°C

Skin samples ($n = 6$) were mounted in transport cells, pre-equilibrated for 2 h in 0.15 M PBS of pH 7.4, in the absence of electrical current, whereafter the current was switched on. Subsequently, the voltage wave was sampled at 1 min intervals, for a total duration of 65 min. From these data the resistances, R_1 and R_2 , and the capacitances, C_1 and C_2 , were evaluated and plotted versus time.

2.4.2. Measurements during heating-cooling cycles

After pre-equilibration of the skin samples in 0.15 M PBS pH 7.4 for 2 h in the absence of current, the temperature of the skin was raised and subsequently reduced at a rate of 2.5 K min⁻¹. The stratum corneum samples ($n = 4-6$) were subjected to three temperature cycles based on previously detected thermal transitions [13,14] and in Bouwstra JA et al., 1994 (unpublished observations): Cycle (1): 20–45–20°C; Cycle (2): 20–75–20°C and Cycle (3): 20–95–20°C.

Throughout the entire heating-cooling cycles measurements as described in 2.4.1. were carried out at 1 min intervals. Recovery from the heat and current treatment was studied by measurement of the electrical properties during the cooling-down part of the temperature cycles.

2.5. Current delivery

Measurements of the resistance and capacitance properties of human stratum corneum at a variable temperature were carried out at two different current densities: 13 $\mu\text{A cm}^{-2}$ in one set of experiments and 130 $\mu\text{A cm}^{-2}$ in another set of experiments. The lower current density profile was selected because during its application at 20°C the electrical properties of human stratum corneum remained constant, whereas application of the higher current density at 20°C resulted in a

decrease of the resistances R_1 and R_2 . The current was delivered by a pair of Ag/AgCl plate electrodes.

The 13 $\mu\text{A cm}^{-2}$ current was a pulsed alternating current characterized by a frequency of 500 Hz, a duty cycle of 50%, an amplitude of 13 $\mu\text{A cm}^{-2}$ and a mean current density of 0 mA cm^{-2} . One current pulse cycle consisted of a 5 ms positive (directed from the anatomical surface to the basal region of stratum corneum) square-wave pulse of 13 $\mu\text{A cm}^{-2}$, after which the current source delivered no current for 5 ms. For the next 5 ms the current polarity was reversed (negative) and a 13 $\mu\text{A cm}^{-2}$ current was applied. Thereafter the current was switched off for another 5 ms.

The 130 $\mu\text{A cm}^{-2}$ current was essentially constant. One current cycle consisted of a positive current pulse of 130 $\mu\text{A cm}^{-2}$ for 100 ms, followed by 1 ms of zero current application.

2.6. Voltage waveform analysis

The voltage difference across stratum corneum was measured by a separate set of Ag/AgCl bar electrodes positioned at a distance of 2 mm from each of the skin surfaces. The voltage wave was sampled at 1 min intervals. The decay parts of the voltage waves were subjected to a least squares non-linear regression computer programme, which was developed in the Central Electronics Department of the Gorlaeus Laboratories (Leiden University, Netherlands) and which was based on the Levi-Marquardt algorithm [15]. A bi-exponential equation Eq. (1) was found to describe the time dependence of the voltage across the skin quite satisfactorily, leading to an equivalent electrical circuit of human stratum corneum consisting of two R||C-circuits in series: $R_1||C_1$ and $R_2||C_2$.

$$V(t) = V_1 \exp\left(-\frac{t}{\tau_1}\right) + V_2 \exp\left(-\frac{t}{\tau_2}\right) + V_\infty \quad (1)$$

In Eq. (1) V_1 and V_2 represent the voltage decay across the resistances R_1 and R_2 , respectively, V_∞ is a residual potential, defined as: $\lim_{t \rightarrow \infty} V(t) = V_\infty$, τ_1 and τ_2 are the time constants, which are equal to the products $R_1 \times C_1$ and $R_2 \times C_2$, respectively. From the best-fit coefficients, V_1 , V_2 , τ_1 and τ_2 , the resistances and capacitances were calculated.

2.7. Calculation of activation energies

Activation energies (E_a) were calculated from the slope of an Arrhenius plot of the natural logarithm of the conductance ($\ln G$) versus the inverse of the absolute temperature ($1/T$) according to the following equation:

$$\ln G = A - E_a/RT \quad (2)$$

in which A represents the intercept, R is the universal gas constant, and in which the conductance G is the reciprocal of the total resistance of stratum corneum; ($1/G = R_1 + R_2$).

3. Results

3.1. Isothermal studies of the resistances and capacitances at 20°C

3.1.1. 13 $\mu\text{A cm}^{-2}$

The initial values of the series resistances R_1 and R_2 measured at a current density of 13 $\mu\text{A cm}^{-2}$ were 21.6 ± 5.4 and $36.7 \pm 3.1 \text{ k}\Omega \text{ cm}^{-2}$, respectively. During current application the resistances remained unchanged and after 65 min the values of R_1 and R_2 were 20.0 ± 4.4 and $39.3 \pm 2.8 \text{ k}\Omega \text{ cm}^{-2}$, respectively (Fig. 1a).

After pre-equilibration the series capacitances C_1 and C_2 were $14.4 \pm 1.7 \times 10^{-9}$ and $38.3 \pm 5.4 \times 10^{-9} \text{ F cm}^{-2}$, respectively. Throughout current application both C_1 and C_2 remained constant and their values after 65 min of current application were 16.2 ± 0.8 and $41.4 \pm 3.1 \times 10^{-9} \text{ F cm}^{-2}$, respectively (Fig. 1b).

3.1.2. 130 $\mu\text{A cm}^{-2}$

The initial resistances R_1 and R_2 measured at a current density of 130 $\mu\text{A cm}^{-2}$ were 10.9 ± 7.5 and $17.6 \pm 2.6 \text{ k}\Omega \text{ cm}^{-2}$, respectively, which is about two times lower than the resistances measured at a current

density of 13 $\mu\text{A cm}^{-2}$. During continuation of current application, the resistances gradually decreased. The decrease of R_1 was most rapid during the first 15 min of application, whereas R_2 continued to decrease at a slow rate during the whole length of the experiment (65 min) (Fig. 1a). After 65 min R_1 and R_2 were 4.8 ± 0.1 and $12.9 \pm 1.4 \text{ k}\Omega \text{ cm}^{-2}$, respectively.

The initial capacitances C_1 and C_2 were $22.7 \pm 7.9 \times 10^{-9}$ and $22.5 \pm 13.8 \times 10^{-9} \text{ F cm}^{-2}$, respectively. During continuation of the current no significant changes in the values of neither C_1 nor C_2 were found; the values of C_1 and C_2 after 65 min were 19.6 ± 5.7 and $26.2 \pm 17.8 \times 10^{-9} \text{ F cm}^{-2}$, respectively (Fig. 1b).

3.2. Temperature dependence of the effects of current density on the resistances and capacitances

The temperature profiles of the resistances and capacitances at both 13 and 130 $\mu\text{A cm}^{-2}$ were characterized by three main events, occurring within the following three temperature intervals:

- (1) A lower interval, from 20 to about 60°C at 13 $\mu\text{A cm}^{-2}$ and from 20 to about 50°C at 130 $\mu\text{A cm}^{-2}$;
- (2) a middle interval, from 60 to about 75°C at 13 $\mu\text{A cm}^{-2}$ and from 50 to about 75°C at 130 $\mu\text{A cm}^{-2}$;
- (3) a higher interval, from 75 to 95°C for both current densities.

For reasons of clarity, these temperature intervals will be discussed separately.

3.2.1. Lower temperature interval

The lower temperature interval at 13 $\mu\text{A cm}^{-2}$ fell between 20 and 60°C, while at 130 $\mu\text{A cm}^{-2}$ the upper temperature had shifted 10° downwards to 50°C. At both the 13 and 130 $\mu\text{A cm}^{-2}$ current densities, the lower temperature interval was characterized by a slow decrease of the resistances R_1 and R_2 (Fig. 2a,b), which was accompanied by a slow increase of the capacitances C_1 and C_2 (Fig. 3a,b). At both current densities the resistances at the upper end of the temperature interval were about two times lower than the initial resistances: at 13 $\mu\text{A cm}^{-2}$ R_1 decreased from 15.2 ± 4.7 to $7.7 \pm 6.0 \text{ k}\Omega \text{ cm}^{-2}$ and R_2 from 52.1 ± 18.7 to $33.3 \pm 8.4 \text{ k}\Omega \text{ cm}^{-2}$; at 130 $\mu\text{A cm}^{-2}$ R_1 decreased from 9.4 ± 2.6 to $4.7 \pm 0.6 \text{ k}\Omega \text{ cm}^{-2}$ and R_2 from 19.6 ± 3.2 to $10.8 \pm 1.2 \text{ k}\Omega \text{ cm}^{-2}$. The stratum corneum conductances measured over the lower temperature interval gave rise to a linear Arrhenius plot for each of the two current densities, yielding an activation energy of $5.41 \pm 0.72 \text{ kcal mol}^{-1}$ at 13 $\mu\text{A cm}^{-2}$ and a 15-times smaller activation energy of $0.37 \pm 0.03 \text{ kcal mol}^{-1}$ at 130 $\mu\text{A cm}^{-2}$ (Fig. 4).

3.2.2. Middle temperature interval

The middle temperature interval was characterized by a sudden drop of the resistances (Fig. 1a,b). More-

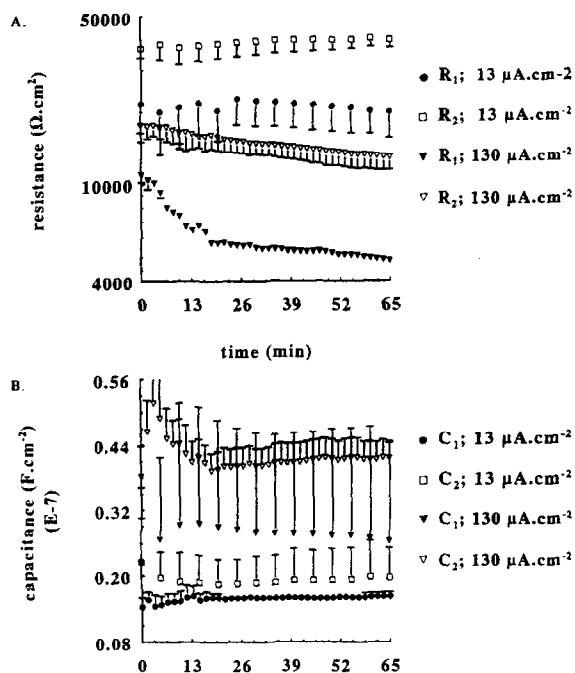


Fig. 1. Effects of current densities varying from 13 to 130 $\mu\text{A cm}^{-2}$ on the resistances (A) and capacitances (B) of human stratum corneum at 20°C. Data represent mean \pm S.D. of $n = 6$ samples.

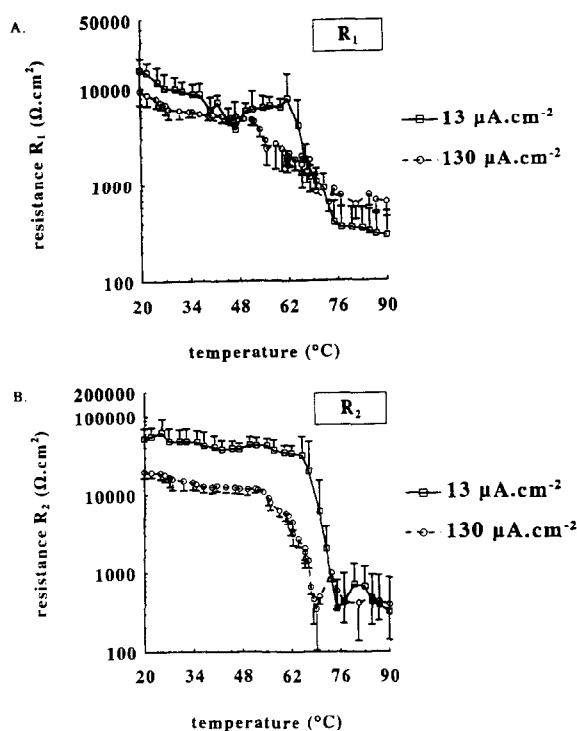


Fig. 2. Thermal dependence of human stratum corneum resistances at two current densities. (A) Thermal dependence of R_1 ; (B) Thermal dependence of R_2 . Data represent mean \pm S.D. of $n = 6$ samples.

over, the Arrhenius plots obtained for the middle temperature interval was characterized by an abrupt increase of their slopes (Fig. 4). The middle temperature interval fell between 60 and 76°C at $13 \mu\text{A} \cdot \text{cm}^{-2}$ and between 50 and 75°C , at $130 \mu\text{A} \cdot \text{cm}^{-2}$. Within these intervals the resistances dropped steeply, approaching the resistance of pure buffer ($0.06 \pm 0.04 \text{ k}\Omega \cdot \text{cm}^{-2}$) at the upper temperature; at $13 \mu\text{A} \cdot \text{cm}^{-2}$ R_1 dropped from 7.7 ± 6.0 to $0.3 \pm 0.3 \text{ k}\Omega \cdot \text{cm}^{-2}$ and R_2 from 33.3 ± 8.4 to $0.3 \pm 0.6 \text{ k}\Omega \cdot \text{cm}^{-2}$; at $130 \mu\text{A} \cdot \text{cm}^{-2}$ R_1 dropped from 4.7 ± 0.6 to $0.6 \pm 0.2 \text{ k}\Omega \cdot \text{cm}^{-2}$ and R_2 from 10.8 ± 1.2 to $0.4 \pm 0.2 \text{ k}\Omega \cdot \text{cm}^{-2}$.

At both current densities the drop of the resistances within the middle temperature interval was accompanied by an increase of the capacitances (Fig. 3a,b). At $13 \mu\text{A} \cdot \text{cm}^{-2}$ a slight increase of C_1 around 60°C was observed. C_1 increased from $1.9 \pm 0.8 \times 10^{-9}$ to $6.0 \pm 3.4 \times 10^{-9} \text{ F} \cdot \text{cm}^{-2}$ and C_2 gradually increased from $19.5 \pm 14.9 \times 10^{-9}$ to $130.2 \pm 82.9 \times 10^{-9} \text{ F} \cdot \text{cm}^{-2}$. At $130 \mu\text{A} \cdot \text{cm}^{-2}$, the increase in C_1 and C_2 was more pronounced than at $13 \mu\text{A} \cdot \text{cm}^{-2}$. C_1 increased from $4.2 \pm 0.5 \times 10^{-9}$ to $6.0 \pm 3.4 \times 10^{-9} \text{ F} \cdot \text{cm}^{-2}$ and C_2 from $33.1 \pm 5.2 \times 10^{-9}$ to $211.1 \pm 70.4 \times 10^{-9} \text{ F} \cdot \text{cm}^{-2}$.

3.2.3. Higher temperature interval

For both current densities, the stratum corneum resistances remained fairly constant at higher temperatures (Fig. 2a,b). Interestingly, beyond approximately

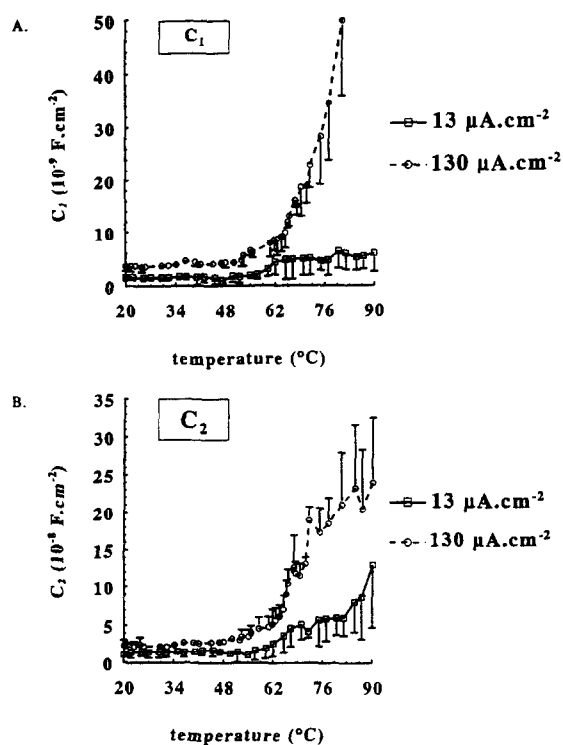


Fig. 3. Thermal dependence of human stratum corneum capacitances. (A) Thermal dependence of C_1 ; (B) Thermal dependence of C_2 . Data represent mean \pm S.D. of $n = 6$ samples.

75°C the two $R_2(T)$ plots for 13 and $130 \mu\text{A} \cdot \text{cm}^{-2}$ converged around $0.6 \text{ k}\Omega \cdot \text{cm}^{-2}$. Within the higher temperature interval the slope of the Arrhenius plots at both current densities was close to zero (Fig. 4).

At $13 \mu\text{A} \cdot \text{cm}^{-2}$ the capacitance C_1 only tended to increase slightly around 60°C and subsequently remained almost constant, whereas C_2 also started to increase around 60°C , but continued to increase sharply up to 95°C . At $130 \mu\text{A} \cdot \text{cm}^{-2}$ both C_1 and C_2 started to rise rapidly at around 50°C and continued to increase to a temperature of 95°C .

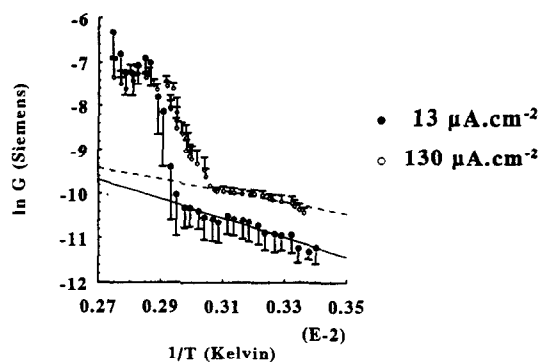


Fig. 4. Arrhenius plot of the electrical conductance of human stratum corneum at two current densities. Data represent mean \pm S.D. of $n = 6$ samples.

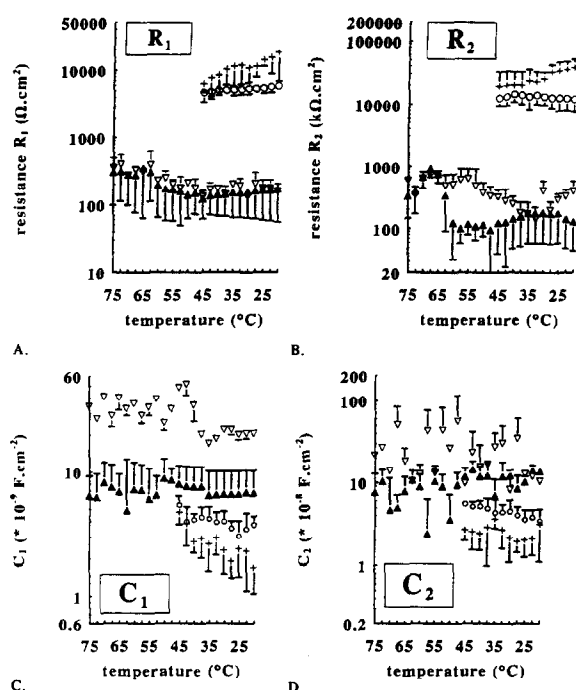


Fig. 5. Reversibility of the electrical properties of human stratum corneum. The electrical properties were measured during the cooling parts of heating-cooling cycles 1 (maximum temperature of 45°C) and 2 (maximum temperature of 75°C). Data represent mean \pm S.D. of $n = 6$ samples. (A) resistance R_1 ; (B) resistance R_2 ; (C) capacitance C_1 and (D) capacitance C_2 . + 45°C, 13 $\mu\text{A}\cdot\text{cm}^{-2}$; ○ 45°C, 130 $\mu\text{A}\cdot\text{cm}^{-2}$; ▲ 75°C, 13 $\mu\text{A}\cdot\text{cm}^{-2}$; ▽ 75°C, 130 $\mu\text{A}\cdot\text{cm}^{-2}$.

3.3. Thermal reversibility of the effects of current density on resistances and capacitances

The electrical properties of human stratum corneum during the cooling-down conditions of the heating-cooling cycles are described for both current densities used (13 and 130 $\mu\text{A}\cdot\text{cm}^{-2}$).

3.3.1. 13 $\mu\text{A}\cdot\text{cm}^{-2}$

During cooling from a temperature of 45°C (cycle 1) at 13 $\mu\text{A}\cdot\text{cm}^{-2}$ a gradual increase of the resistances R_1 and R_2 was observed (Fig. 5a,b). At 20°C R_1 and R_2 were similar to their values before heating: 18.2 ± 11.3 and 38.3 ± 13.6 $\text{k}\Omega\cdot\text{cm}^{-2}$, respectively. Moreover, the capacitances C_1 and C_2 recovered to values which were not significantly different from their initial values measured before heating: $1.8 \pm 0.6 \times 10^{-9}$ and $3.1 \pm 1.9 \times 10^{-9}$ $\text{F}\cdot\text{cm}^{-2}$, respectively (Fig. 5c,d).

After heating to maximum temperatures of 75 and 95°C (cycle 2 and 3), the resistances remained below 0.6 $\text{k}\Omega\cdot\text{cm}^{-2}$ and continued to fluctuate around this level when temperatures were decreased to 20°C (Fig. 5a,b). The capacitances C_1 and C_2 did not recover either, but kept fluctuating around values, which were 4–10 times higher than the values before heating (Fig. 5c,d).

3.3.2. 130 $\mu\text{A}\cdot\text{cm}^{-2}$

After raising the temperature to 45°C and subsequent cooling down to 20°C, both R_1 and R_2 obtained values of 5.9 ± 0.8 and 12.0 ± 4.3 $\text{k}\Omega\cdot\text{cm}^{-2}$, respectively, at 20°C. These values were not significantly different from their initial values at 20°C (Fig. 5a,b). C_1 and C_2 gradually increased and reached values of $3.7 \pm 0.6 \times 10^{-9}$ and $3.4 \pm 1.3 \times 10^{-8}$ $\text{F}\cdot\text{cm}^{-2}$ respectively at 20°C, which are not significantly different from their values before heating (Fig. 5c,d).

When temperatures were decreased from 75 or 95 to 20°C (cycle 2 or 3) the resistances did not recover at all, but remained below 1 $\text{k}\Omega$. The capacitances did not recover either (Fig. 5c,d).

4. Discussion

4.1. Effects of current density on resistances and capacitances at 20°C

During application of a current of 13 $\mu\text{A}\cdot\text{cm}^{-2}$ at 20°C both the resistances and capacitances remained constant (Fig. 1a,b). The voltage across the skin samples resulting from the 13 $\mu\text{A}\cdot\text{cm}^{-2}$ remained at a constant level of around 1 V. These results show that a continued application 13 $\mu\text{A}\cdot\text{cm}^{-2}$ does not cause changes of the electrical properties of human stratum corneum. This is in agreement with a study on the current-voltage relationship of human skin, which has demonstrated a linear current-voltage relationship and thus a constant skin resistance at current densities lower than 15 $\mu\text{A}\cdot\text{cm}^{-2}$ [16].

On application of 130 $\mu\text{A}\cdot\text{cm}^{-2}$, two major differences were observed, compared to the resistance measurements at 13 $\mu\text{A}\cdot\text{cm}^{-2}$ (Fig. 1a): Firstly, the resistances measured at the start of current-application were lower by a factor of two than the initial resistances at 13 $\mu\text{A}\cdot\text{cm}^{-2}$. The voltage measured at the start of current-delivery was approximately 10 V. The initial decrease of the resistance during application of the 130 $\mu\text{A}\cdot\text{cm}^{-2}$ occurred beyond the resolution of the voltage-sampling system, which is 10 μs and therefore must be attributed to a very rapid mechanism, most likely based on a direct electrical field effect rather than an indirect effect caused by current. In comparison with a direct electrical field effect, an indirect current related mechanism, such as heat dissipation or interactions of ions (primarily Na^+ and Cl^-) with substructures of the stratum corneum or displacement of structurally important ions such as Ca^{2+} , is expected to decrease the resistance of human stratum corneum more slowly.

Secondly, during application of a current of 130 $\mu\text{A}\cdot\text{cm}^{-2}$ a second slower decrease of the resistances was observed, which was the fastest during the first min of application after which the resistances approached a

rather constant level. Along with the resistance, the voltage across the skin decreased from 10 to 1 V, whereupon it remained virtually constant.

4.2. Effects of current density on the temperature dependence of the resistances and capacitances

The heating-cooling cycles applied in the present study were based on previous knowledge about the thermal transitions in human stratum corneum, detected by differential scanning calorimetric and X-ray diffraction studies [12–14].

4.3. Heating from 20 to 95°C

4.3.1. $13 \mu\text{A cm}^{-2}$

From 20 to 60°C, a gradual decrease of the resistances and a gradual increase of the capacitances was observed, which was not interrupted by a notable change around 40°C. At this temperature, the lateral orthorhombic lipid packing changes into a hexagonal lipid packing [14]. Thus the present observation indicates that the transition from an orthorhombic arrangement of the lipids to a hexagonal arrangement has no significance for the electrical properties of human stratum corneum.

Below 60°C, the Arrhenius plot yielded a straight line and a single activation energy was calculated, suggesting that the observed conductance increase from 20 to 60°C is reversible. The activation energy of $5.4 \pm 0.7 \text{ kcal mol}^{-1}$ is in the same order of magnitude to the activation energy determined for K^+ diffusion through in an aqueous medium [17]. Apparently, the ions travel along highly conductive pathways. The presence of highly conductive pathways is also suggested by the resistance of human stratum corneum, which is relatively low (approximately $60 \text{ k}\Omega \text{ cm}^{-2}$) compared to the resistance of black lipid films ($1\text{--}10 \text{ M}\Omega \text{ cm}^{-2}$) [18].

The gradual changes of the electrical properties ended abruptly at 60°C, at which temperature the resistances started to decrease rapidly while the capacitances started to increase. At the same temperature the slope of the Arrhenius-plot also changed abruptly, indicating a disturbance of the skin barrier structure. Between 60 and 75°C, an almost complete loss of the barrier function (resistances) was observed, and at 75°C the resistances were only 10-times higher than the resistance of pure buffer. The drastic changes in the electrical properties between 60 and 75°C were indicative of considerable structural changes. Hence, calculation of activation energies was impossible. Interestingly, this thermal transition of the electrical resistances and capacitances corresponds well to the second thermal transition, as observed with differential scanning calorimetry of human stratum corneum, which has been attributed to lipids, not attached to protein. Further investigation of

this thermal transition by X-ray diffraction has shown that this transition is caused by a disordering of the intercellular lamellar lipid phase [14] and Bouwstra JA et al., 1994 (unpublished results), cf 2.4.2.

The main decrease of the resistances occurred within the temperature interval of the third lipid thermal transition and the resistances only slightly decreased at higher temperatures, indicating that the non-protein bound intercellular lipids are mainly responsible for the high resistance of stratum corneum against ion transport. However, the capacitances continued to increase from 75 to 95°C, suggesting that the charge storage capacity of human stratum corneum also depends on protein-bound lipids, which undergo a thermal transition at around 85°C [13,14].

4.3.2. $130 \mu\text{A cm}^{-2}$

From 20 to 55°C the resistances and capacitances changed gradually and, similar to the measurements at $13 \mu\text{A cm}^{-2}$, no influence of the thermal transition at 45°C was observed. From 20 to 55°C, the Arrhenius-plot was characterized by a straight line, suggesting that the decrease of the resistance in this temperature interval was reversible. The activation energy calculated from the slope of the Arrhenius-plot was about 10-times lower than the activation energy at $13 \mu\text{A cm}^{-2}$. Apparently, the number and/or the dimensions of ion pathways are increased under the influence of an electrical field.

The thermal transition of the resistances and capacitances started at a temperature, which was about 10°C lower than at $13 \mu\text{A cm}^{-2}$. Since it might be assumed that the thermal transition at $13 \mu\text{A cm}^{-2}$ was associated with a gel-liquid phase transition of the intercellular lipid lamellae, the downward shift of the thermal transition of the electrical properties at $130 \mu\text{A cm}^{-2}$ corresponds most likely with a downward shift of the gel-liquid lipid phase transition temperature. These results demonstrate that a current density of $130 \mu\text{A cm}^{-2}$ is able to reduce the electrical resistances, the activation energy of ion transport across the skin barrier as well as to increase the capacitances by modifying the structure of the intercellular lipid lamellae.

Expansion of the area of phospholipid membranes has been found to occur under the influence of electrical fields [19]. Moreover, the resistance of phospholipid membranes was also found to decrease. Similarities between the thermo-electrical behaviour of phospholipid membranes and human stratum corneum, such as a non-linear voltage-current relationship and a downward shift of the transition temperature of the electrical resistance under the influence of an electrical field, suggest that the mechanism behind this similar behaviour is also identical in both cases [7,19]. A possible mechanism explaining such a field effect on both human stratum corneum and phospholipid membranes

could be a polarization of the lipid headgroups, followed by a disruption of the lipid ordering.

4.4. Thermal reversibility

The resistances and capacitances at $13 \mu\text{A cm}^{-2}$ recovered after stratum corneum was heated to 45°C and subsequently cooled-down to 20°C . However, at temperatures exceeding 75°C no reversibility was observed regardless of the current density used. Therefore, beyond 75°C as well as upon subsequent cooling, the presence of the electrical field is completely overruled by the thermally induced changes in the stratum corneum and the thermal parameter does not give any additional information, but is at the most indicative of changes in lipid packing. Hence, above the gel-liquid lipid phase transition, the temperature ceases to contribute as an auxiliary parameter.

The observation that the thermal transition between 60 and 75°C at $13 \mu\text{A cm}^{-2}$ is irreversible, corresponds to observations made by X-ray diffraction, which have shown that the gel-liquid lipid thermal transition, which takes place at a temperature of approximately 75° at $0 \mu\text{A cm}^{-2}$ and $13 \mu\text{A cm}^{-2}$ and at around 60°C at $130 \mu\text{A cm}^{-2}$, leads to a completely different small-angle diffraction pattern after cooling than before heating [14].

References

- [1] Cullander C, Guy RH. Transdermal delivery of peptides and proteins. *Adv. Drug Delivery Rev.* 1992;8:291–329.
- [2] Meyer BR, Kreis W, Eschbach J, O'Mara V, Rosen S, Sibalis D. Successful administration of therapeutic doses of a polypeptide to normal human volunteers. *Clin. Pharmacol. Ther.* 1988;44:607–612.
- [3] Siddiqui O, Sun Y, Lui JC, Chien YW. Facilitated transdermal transport of insulin. *J. Pharm. Sci.* 1987;76:341–345.
- [4] Kumar S, Char H, Patel S et al. In vivo transdermal iontophoretic delivery of growth hormone releasing factor GRF (1–44) in hairless guinea pigs. *J. Control. Rel.* 1991;18:213–220.
- [5] Knoblauch P, Moll F. In vitro pulsatile and continuous transdermal delivery of buserelin by iontophoresis. *J. Control. Rel.* 1993;26:203–212.
- [6] Kontturi K, Murtomäki L, Hirvonen J, Paronen P, Urtti A. Electrochemical characterization of human skin by impedance spectroscopy: the effect of penetration enhancers. *Pharm. Res.* 1993;10:381–385.
- [7] Lykken DT. Square-wave analysis of skin impedance. *Psychophysiology* 1971;7:262–275.
- [8] Craane-van Hinsberg WHM, Boddé HE, Verhoef J, Bax LJ, Junginger HE. Evaluation of a pulsed current and high-frequency voltage sampling system designed to study transdermal peptide iontophoresis and skin impedance. *J. Control. Rel.* 1992;21:212–213.
- [9] Craane-van Hinsberg WHM. Transdermal peptide iontophoresis: a mechanistic study of electrical skin barrier perturbation and transport enhancement. Ph.D. Thesis, Leiden University, Leiden, 1995, pp. 41–52.
- [10] Oh SY, Leung L, Bommannan D, Guy RH, Potts RO. Effect of current, ionic strength and temperature on the electrical properties of skin. *J. Control. Rel.* 1993;27:115–125.
- [11] Craane-van Hinsberg WHM, Verhoef JC, Junginger HE, Boddé HE. Thermo-electrical analysis of the human skin barrier. *Thermochim. Acta* 1995;248:303–318.
- [12] Craane-van Hinsberg WHM, Bax L, Flinterman NHM, Verhoef JC, Junginger HE, Boddé HE. Iontophoresis of a model peptide across human skin in vitro: effects of iontophoresis protocol, pH and ionic strength on peptide flux and skin impedance. *Pharm. Res.* 1994;11:1296–1300.
- [13] Potts RO, Golden GM, Francoeur ML, Mak VHW, Guy RH. Mechanism and enhancement of solute transport across the stratum corneum. *J. Control. Rel.* 1991;15:249–260.
- [14] Bouwstra JA, Gooris GS, van der Spek JA, Bras W. Lipid arrangements in human stratum corneum. *Prog. Colloid Polym. Sci.* 1992;88:110–122.
- [15] Kurzweil P. Modellanalyse leichtgemacht. MC, 1990, pp. 124–131.
- [16] Kasting GB, Bowman LA. Electrical analysis of fresh human skin: A comparison with frozen skin. *Pharm. Res.* 1990;7:1141–1146.
- [17] Stein WD. *Transport and Diffusion Across Cell Membranes*. Academic Press, NY, 1986.
- [18] Chernomordik LV, Sukharev SI, Abidor IG, Chizmadzhev YA. Breakdown of lipid membranes in an electrical field. *Biochim. Biophys. Acta* 1983;736:203–213.
- [19] Sugár IP. A theory of the electric field-induced phase transition of phospholipid bilayers. *Biochim. Biophys. Acta* 1979;556:72–85.